J|A|C|S
ARTICLES
Published on Web 09/17/2005

Intermolecular Packing and Alignment in an Ordered β-Hairpin Antimicrobial Peptide Aggregate from 2D Solid-State NMR

Ming Tang,[†] Alan J. Waring,[‡] and Mei Hong*,[†]

Contribution from the Department of Chemistry, Iowa State University, Ames, Iowa 50011, and Department of Medicine, University of California at Los Angeles School of Medicine, Los Angeles, California 90095

Received April 25, 2005; E-mail: mhong@iastate.edu

Abstract: The aggregation and packing of a membrane-disruptive β-hairpin antimicrobial peptide, protegrin-1 (PG-1), in the solid state are investigated to understand its oligomerization and hydrogen-bonding propensity. Incubation of PG-1 in phosphate buffer saline produced well-ordered nanometer-scale aggregates, as indicated by ^{13}C and ^{15}N NMR line widths, chemical shifts, and electron microscopy. Two-dimensional ^{13}C and ^{1}H spin diffusion experiments using C-terminus strand and N-terminus strand labeled peptides indicate that the β-hairpin molecules in these ordered aggregates are oriented parallel to each other with like strands lining the intermolecular interface. In comparison, disordered and lyophilized peptide samples are randomly packed with both parallel and antiparallel alignments. The PG-1 aggregates show significant immobilization of the Phe ring near the β-turn, further supporting the structural ordering. The intermolecular packing of PG-1 found in the solid state is consistent with its oligomerization in lipid bilayers. This solid-state aggregation approach may be useful for determining the quaternary structure of peptides in general and for gaining insights into the oligomerization of antimicrobial peptides in lipid bilayers in particular.

Introduction

Protegrin-1 (PG-1) is a small β-hairpin peptide from porcine leukocytes that has potent and broad-spectrum antimicrobial activities.[1] Its minimum inhibitory concentrations lie in the range of a few micrograms per milliliter, more than 2 orders of magnitude stronger than existing antibiotics such as vancomysin.[2] PG-1 carries out this remarkably efficient microbicidal function by destroying the cell membranes of the target organisms. Yet, how the peptide interacts with lipid bilayers on a molecular level, and what properties of the amino acid sequence of the peptide endow its potent and selective membrane-disruptive ability, remain a mystery. Understanding PG-1 structure can shed light on the structure−function relationships of a large class of similar β-sheet antimicrobial peptides.[3]

Using solid-state NMR chemical shift anisotropy and dipolar coupling measurements, we recently found that PG-1 is immobilized in POPC bilayers, where the lipid acyl chains contain 16−18 carbons, but undergoes rigid-body uniaxial rotation in DLPC bilayers, where the lipid chains have only 12 carbons.[4] The immobilization in the biologically relevant membrane thickness of POPC bilayers suggests that the peptide is aggregated. Using ^{19}F spin diffusion NMR, we found that PG-1 is dimerized in POPC bilayers.[5] This prompted questions pertaining to the dimer structure: are the β-hairpins aligned parallel or antiparallel to each other? Which strand of the hairpin forms the dimer interface? Understanding the detailed membrane-bound dimer structure, which is essentially determined by intermolecular hydrogen bonding, is important for deciphering the mechanism of action of the peptide. Because PG-1 is highly cationic, similar to most antimicrobial peptides,[6] the dimer structure can also provide useful insights into the energetic driving force for the insertion of PG-1 into the hydrophobic membrane.

The crystal structures of two β-sheet antimicrobial peptides outside the lipid or detergent environments have been determined to understand the oligomerization and mechanisms of action of these peptides in the membrane.[7,8] It was found that these β-sheet peptides form dimers in the crystal, stabilized by a combination of hydrophobic interactions and hydrogen bonds. Because the crystal structure of PG-1 is not available, an alternative approach for gaining insights into the oligomerization of this peptide in the membrane is to create well-ordered and lipid-free peptide aggregates whose intermolecular packing can be determined by solid-state NMR. Studying the structure of lipid-free ordered aggregates has the practical advantages that it has high sensitivities due to the avoidance of lipid dilution and that it does not suffer from the dynamic disorder common to membrane systems. Further, the solid-state aggregate structure

[†] Iowa State University.
[‡] University of California at Los Angeles School of Medicine.

(1) Bellm, L.; Lehrer, R. I.; Ganz, T. *Expert Opin. Invest. Drugs* **2000**, *9*, 1731−1742.
(2) Muhle, S. A.; Tam, J. P. *Biochemistry* **2001**, *40*, 5777−5785.
(3) Epand, R. M.; Vogel, H. J. *Biochim. Biophys. Acta* **1999**, *1462*, 11−28.
(4) Buffy, J. J.; Waring, A. J.; Lehrer, R. I.; Hong, M. *Biochemistry* **2003**, *42*, 13725−13734.
(5) Buffy, J. J.; Waring, A. J.; Hong, M. *J. Am. Chem. Soc.* **2005**, *127*, 4477−4483.
(6) Hancock, R. E.; Lehrer, R. *Trends Biotechnol.* **1998**, *16*, 82−88.
(7) Hoover, D. M.; Rajashankar, K. R.; Blumenthal, R.; Puri, A.; Oppenheim, J. J.; Chertov, O.; Lubkowski, J. *J. Biol. Chem.* **2000**, *275*, 32911−32918.
(8) Hill, C. P.; Yee, J.; Selsted, M. E.; Eisenberg, D. *Science* **1991**, *251*, 1481−1485.

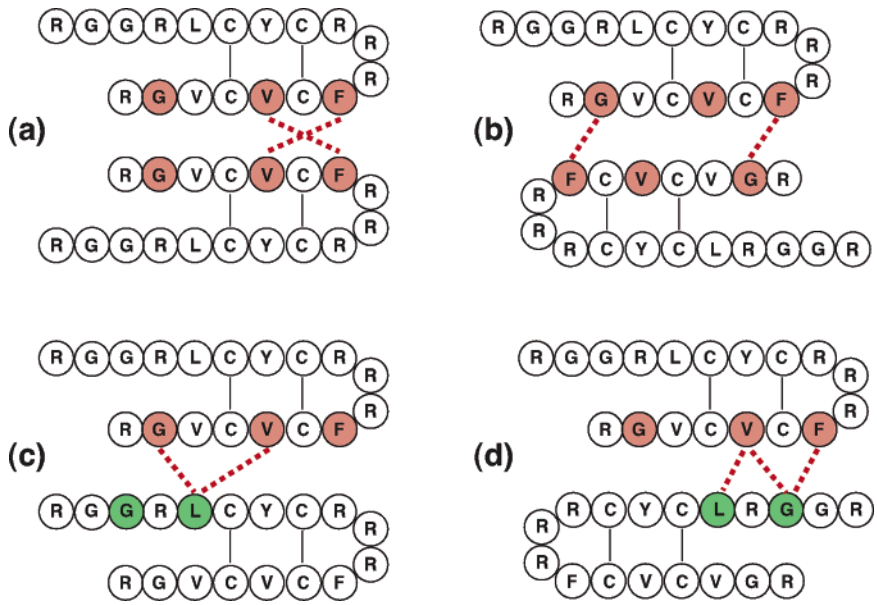

Figure 1. Schematics of possible modes of packing of the β-hairpin peptide PG-1. (a) NCCN parallel packing. (b) NCCN antiparallel packing. (c) NCNC parallel packing. (d) NCNC antiparallel packing. Colored residues indicate uniformly ^{13}C,^{15}N-labeled residues used in this study. Dashed lines indicate expected short intermolecular distances.

can be compared with independently determined membrane-bound oligomeric structure to shed light on the importance of various noncovalent interactions and the environment to peptide oligomerization.

In addition to antimicrobial peptides, other examples of β-strand peptide oligomerization include the amyloid peptide fibrils found in neurodegenerative diseases such as the Alzheimer's disease.[9] The packing and high-resolution structure of the Alzheimer's β-peptide Aβ_{1-40} have recently been determined using solid-state NMR.[10] Whether PG-1 can form similar extended fibrils is not obvious, because the 18-residue disulfide-linked peptide has a much smaller shape anisotropy than typical amyloid-forming peptides, making the free energy reduction of oligomerization less significant than the longer β-strand peptides. The β-hairpin fold of PG-1 also presents an additional degree of complexity and novelty to the oligomerization: because the two strands of the hairpin share intramolecular hydrogen bonds in the plane of the β-sheet, oligomerization can occur either with like strands or with unlike strands lining the intermolecular interface.

Two general NMR strategies are available for determining the oligomeric structure of peptides. The first involves distance measurements on site-specifically labeled samples.[11−13] A number of solid-state NMR techniques already exist for measuring site-specific distances with high accuracy.[14,15] However, the success of this approach depends crucially on the labeling positions, otherwise one may not be able to extract measurable distances even for closely packed molecules. The second approach bypasses this difficulty by increasing the number of labeled sites in the peptide and uses more qualitative methods such as spin diffusion [16] to determine the proximity of spins between different molecules.[17,18]

In this work, we show that β-hairpin PG-1 can indeed form ordered aggregates on the tens-of-nanometer scale by suitable solution incubation, and we have determined the molecular packing and alignment in these aggregates using 2D ^{13}C and ^{1}H spin diffusion NMR. Several residues in PG-1 are uniformly labeled in ^{13}C and ^{15}N. Distance-dependent ^{13}C and ^{1}H spin diffusion produces cross-peaks in the 2D spectra whose intensities provide semiquantitative constraints on the intermolecular distances. In this way, we have determined both the identity of the β-strand lining the intermolecular interface and the mutual alignment of the strands.

Materials and Methods

Uniformly ^{13}C,^{15}N-labeled Gly, Leu, Phe, and Val were purchased from Isotec (Miamisburg, OH) and Cambridge Isotope Laboratory (Andover, MA) and converted to Fmoc derivatives by Synpep Corp. (Dublin, CA). PG-1 (NH_2−RGGRLCYCRRRFCVCVGR−$CONH_2$) was synthesized using Fmoc solid-phase peptide synthesis protocols and purified by HPLC as described previously.[19] The labeled amino acids were incorporated at residues F_{12}, V_{14}, and G_{17} on one sample, and G_3 and L_5 on another sample (Figure 1).

Preparation of PG-1 Samples. Ordered PG-1 aggregates were prepared by dissolving the purified and lyophilized peptide in pH 7 phosphate buffer saline (PBS) containing 10 mM phosphates and 100 mM sodium chloride. The concentration of the peptide was typically 2−3 mM. The solution was incubated at room temperature for 2−3 weeks with gentle shaking. The solution was then centrifuged, and the precipitate was collected and dried for ~8 h before being packed into NMR rotors for magic-angle spinning (MAS) experiments. Mixed aggregates and 20% diluted aggregate samples were prepared by co-incubating appropriate amounts of the starting compounds in the PBS

(9) Murphy, R. M. *Annu. Rev. Biomed. Eng.* **2002**, *4*, 155−174.
(10) Petkova, A. T.; Ishii, Y.; Balbach, J. J.; Antzutkin, O. N.; Leapman, R. D.; Delaglio, F.; Tycko, R. *Proc. Natl. Acad. Sci. U.S.A.* **2002**, *99*, 16742−16747.
(11) Balbach, J. J.; Petkova, A. T.; Oyler, N. A.; Antzutkin, O. N.; Gordon, D. J.; Meredith, S. C.; Tycko, R. *Biophys. J.* **2002**, *83*, 1205−1216.
(12) Yang, J.; Weliky, D. P. *Biochemistry* **2003**, *42*, 11879−11890.
(13) Toke, O.; O'Connor, R. D.; Weldeghiorghis, T. K.; Maloy, W. L.; Glaser, R. W.; Ulrich, A. S.; Schaefer, J. *Biophys. J.* **2004**, *87*, 675−687.
(14) Gullion, T.; Schaefer, J. *J. Magn. Reson.* **1989**, *81*, 196−200.
(15) Raleigh, D. P.; Levitt, M. H.; Griffin, R. G. *Chem. Phys. Lett.* **1988**, *146*, 71−76.
(16) Suter, D.; Ernst, R. R. *Phys. Rev. B* **1985**, *32*, 5608−5627.
(17) Tycko, R.; Ishii, Y. *J. Am. Chem. Soc.* **2003**, *125*, 6606−6607.
(18) Lange, A.; Luca, S.; Baldus, M. *J. Am. Chem. Soc.* **2002**, *124*, 9704−9705.
(19) Yamaguchi, S.; Hong, T.; Waring, A.; Lehrer, R. I.; Hong, M. *Biochemistry* **2002**, *41*, 9852−9862.

solution. The untreated PG-1 samples were taken directly from the purified and lyophilized peptide without solution incubation.

Solid-State NMR Experiments. NMR experiments were carried out on a Bruker (Karlsruhe, Germany) DSX-400 spectrometer operating at a resonance frequency of 400.49 MHz for ^{1}H, 100.70 MHz for ^{13}C, and 40.58 MHz for ^{15}N. A triple-resonance MAS probe equipped with a 4 mm spinning module was used for the experiments. Low-temperature experiments were conducted by cooling the bearing air through a Kinetics Thermal Systems XR air-jet sample cooler (Stone Ridge, NY). The temperature was maintained within ±1 K of the desired value, and the spinning speed was regulated to within ±3 Hz. Typical 90° pulse lengths were 5 μs for ^{13}C and ^{15}N and 3.5−4.0 μs for ^{1}H. ^{1}H−^{13}C and ^{1}H−^{15}N cross-polarization (CP) contact times were 0.7 and 1 ms, respectively. Typical recycle delays were 2 s. ^{13}C and ^{15}N chemical shifts were referenced externally to the α-Gly ^{13}C′ signal at 176.4 ppm on the TMS scale and the *N*-acetyl-valine ^{15}N signal at 122.0 ppm on the NH_3 scale, respectively. Secondary shifts were calculated after converting the random coil chemical shift values[20] onto the same scales.

2D ^{1}H-driven ^{13}C spin diffusion (PDSD) and ^{1}H spin diffusion (CHHC) experiments were carried out at a spinning speed of 5.4 kHz to minimize sideband overlap and to avoid rotational resonance effects[15] between directly bonded ^{13}C labels. A ω_1 spectral window of 20 kHz and a maximum t_1 evolution time of 11.2 ms were used. The mixing time τ_{SD} was 400 ms for ^{13}C spin diffusion and 200 μs for ^{1}H spin diffusion. For the CHHC experiment, a short ^{13}C−^{1}H CP contact time τ_{CP} of 120 μs was used before and after the ^{1}H mixing period to ensure site-specific detection of the ^{1}H−^{1}H distances. The short τ_{SD} for the CHHC experiment minimizes the relay mechanism for strong cross-peaks.[21]

The 2D wide-line separation (WISE) experiment[22] was used to measure ^{1}H−^{1}H dipolar couplings in various PG-1 samples. After ^{1}H evolution under ^{1}H−^{1}H and ^{1}H−^{13}C dipolar couplings for a maximum of 0.13 ms, the ^{1}H magnetization is transferred site-specifically to ^{13}C by a 200 μs Lee-Goldburg (LG) CP period.[23,24]

^{13}C−^{1}H dipolar couplings between directly bonded C−H spins were measured using the 2D LG-CP experiment.[25] The evolution time (t_1) is the LG-CP contact time, during which ^{1}H spin diffusion is suppressed by the magic-angle spin lock. At short contact times (<1 ms), only directly bonded ^{13}C−^{1}H dipolar couplings are observed. ^{13}C detection during t_2 resolves these ^{13}C−^{1}H couplings according to the ^{13}C isotropic chemical shifts. The spinning speed was 10 kHz, and the maximum t_1 was 2.56 ms. To achieve polarization transfer, the first sideband matching condition, $\omega_{1C} = \omega_{eff,H} - \omega_r$, was used, where ω_{1C} is the ^{13}C spin-lock field strength and $\omega_{eff,H}$ is the ^{1}H effective spin-lock field strength. Due to the short ^{1}H $T_{1\rho}$ values, which make it difficult to measure small C−H couplings, we used a constant-time version of the experiment where a variable ^{1}H LG spin-lock period was added before CP to make the total ^{1}H spin-lock time constant.[24,26]

^{1}H rotating-frame spin−lattice relaxation times ($T_{1\rho}$) were measured using a ^{13}C-detected ^{1}H LG spin-lock experiment. Again, the use of magic-angle spin lock suppresses ^{1}H spin diffusion so that only the $T_{1\rho}$ of protons directly attached to the ^{13}C is detected. The ^{1}H spin-lock field strength was 70 kHz.

Electron Microscopy. Aliquots of incubated PG-1 solutions were applied to Formvar coated nickel grids. After adsorption for ~2 min, the excess fluid was wicked off and the samples were negatively stained by applying a drop of 1% phosphotungstic acid (PTA; pH 6.2) for <1 min. Excess fluid was wicked off, and grids were air-dried. TEM images were collected using a JEOL 1200EX II scanning and transmission electron microscope (Japan Electron Optics Laboratory, Peabody, MA) at 80 kV and were digitally collected with a Megaview III camera and SIS Pro software (Soft Imaging Systems, Inc., Lakewood, CO).

Results

Figure 1 shows a schematic diagram of the possible modes of intermolecular packing of the β-hairpin PG-1. For simplicity, only two molecules are shown in each model, but the pattern is expected to repeat in a well-ordered aggregate on the tens of nanometer scale. In addition to the possibilities of parallel and antiparallel alignment, the β-hairpins can arrange themselves either with like strands facing each other, NCCN, or with unlike strands facing each other, NCNC. This results in four distinct packing motifs. These different modes of packing can be distinguished with suitably labeled peptides. If the peptide is labeled solely on one strand, then the presence of intermolecular cross-peaks will prove the existence of the like-strand NCCN packing. If such cross-peaks are absent, and NCNC packing is suspected, then a mixture of N-strand-labeled and C-strand-labeled peptide should give rise to intermolecular cross-peaks. To determine whether the strands align in a parallel or antiparallel fashion, the labeling positions on each strand should include both ends. Figure 1 highlights the labeled residues in two PG-1 samples: one incorporates uniformly ^{13}C,^{15}N-labeled F_{12}, V_{14}, and G_{17} (red), while the other contains uniformly labeled G_3 and L_5 (green). The figure also shows the short intermolecular distances expected for each packing motif (dashed lines): F_{12}−V_{14} for NCCN parallel packing (a), F_{12}−G_{17} for NCCN antiparallel packing (b), G_{17}−L_5 and possibly V_{14}−L_5 for NCNC parallel packing (c), and F_{12}−G_3, V_{14}−G_3, and V_{14}−L_5 for NCNC antiparallel packing (d).

Preparation and Characterization of Ordered PG-1 Aggregates. To obtain well-ordered PG-1 aggregates, we incubated the peptide in PBS solution for an extended period of time with gentle agitation. Representative TEM images of the resulting aggregates (Figure 2) show a network of strands that are ~10 nm wide and ~100 nm long. These are shorter and thicker than the amyloid fibrils of Aβ peptides[10] and distinct in morphology. To assess the local order and secondary structure of the aggregates on the subnanometer length scale, we compared the ^{13}C and ^{15}N line widths and chemical shifts of the incubated and untreated peptide. Figure 3a,b shows the ^{13}C CP-MAS spectra of [U-F_{12}, V_{14}, G_{17}] PG-1 in the two different states. Several changes are observed. First, the spectral resolution is much enhanced by incubation: for example, V_{14} Cα and F_{12} Cα became much better resolved, and the C′ peak narrowed. Second, the Cα and C′ peaks in the PG-1 aggregate shifted upfield as compared to the untreated peptide, while the resolved Val Cβ shifted downfield. Based on the known ^{13}C secondary shifts of proteins,[27,28] these indicate that the incubation procedure makes the β-strand conformation of PG-1 more ideal. In comparison, the N-strand labeled peptide, [U-G_3, L_5] PG-1, showed less pronounced chemical shift and line width differ-

(20) Wishart, D. S.; Bigam, C. G.; Holm, A.; Hodges, R. S.; Sykes, B. D. *J. Biomol. NMR* **1995**, *5*, 67−81.
(21) Lange, A.; Seidel, K.; Verdier, L.; Luca, S.; Baldus, M. *J. Am. Chem. Soc.* **2003**, *125*, 12640−12648.
(22) Schmidt-Rohr, K.; Clauss, J.; Spiess, H. W. *Macromolecules* **1992**, *25*, 3273−3277.
(23) Lee, M.; Goldburg, W. I. *Phys. Rev.* **1965**, *140*, A1261−A1271.
(24) Yao, X. L.; Conticello, V. P.; Hong, M. *Magn. Reson. Chem.* **2004**, *42*, 267−275.
(25) vanRossum, B. J.; Forster, H.; deGroot, H. J. M. *J. Magn. Reson.* **1997**, *124*, 516−519.
(26) Tekely, P.; Gerardy, V.; Palmas, P.; Canet, D.; Retournard, A. *Solid State Nucl. Magn. Reson.* **1995**, *4*, 361−367.
(27) Wishart, D. S.; Sykes, B. D.; Richards, F. M. *J. Mol. Biol.* **1991**, *222*, 311−333.
(28) Spera, S.; Bax, A. *J. Am. Chem. Soc.* **1991**, *113*, 5490−5492.

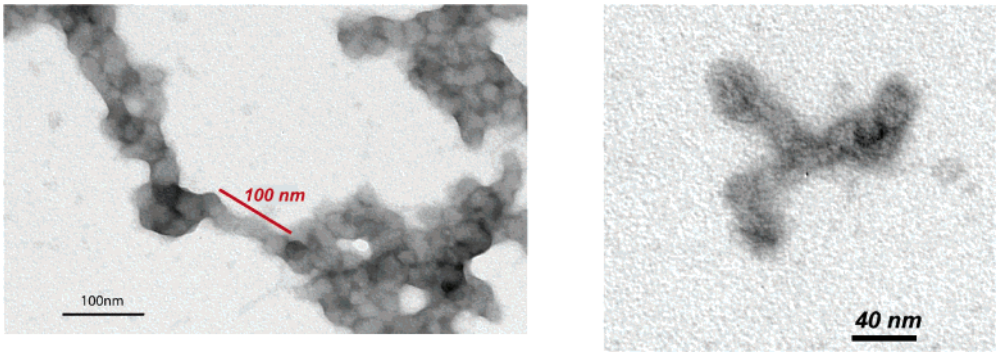

Figure 2. TEM images of PG-1 aggregates incubated from the PBS solution. The aggregates are ~100 nm long and ~10 nm wide.

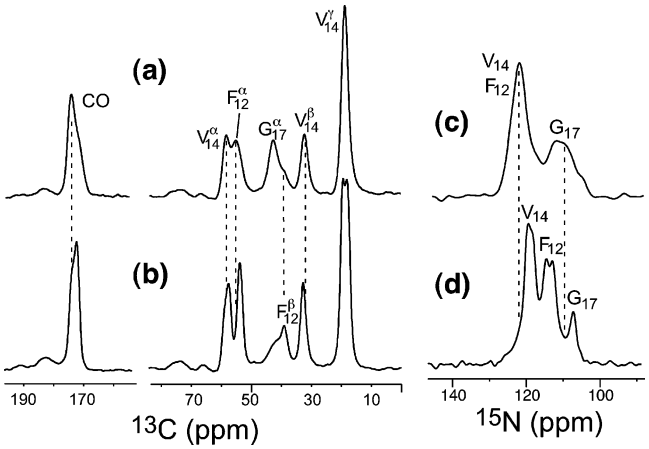

Figure 3. (a,b) ^{13}C MAS spectra of (a) untreated and (b) aggregated [U-F_{12}, V_{14}, G_{17}] PG-1. (c,d) ^{15}N MAS spectra of (c) untreated and (d) aggregated [U-F_{12}, V_{14}, G_{17}] PG-1.

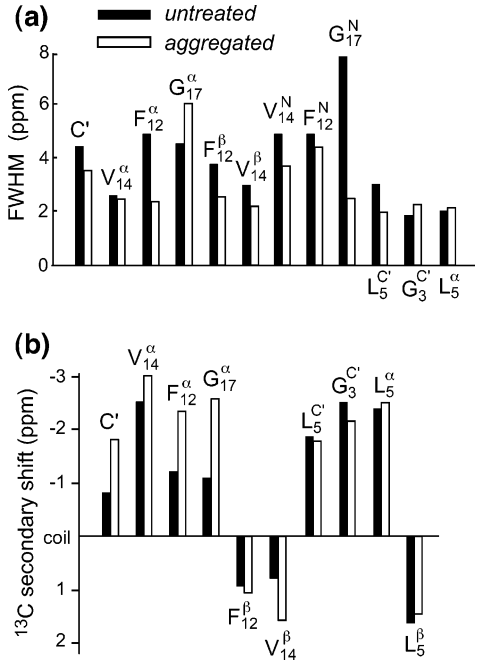

Figure 4. (a) ^{13}C and ^{15}N full widths at half-maximum (fwhm) of untreated (filled) and aggregated (open) PG-1. Smaller line widths indicate a more ordered conformation. (b) ^{13}C secondary shifts of untreated (filled) and aggregated (open) PG-1, calculated as $\Delta_{obs} - \Delta_{rc}$, where Δ_{rc} are the random-coil chemical shifts. Negative Cα and C′ secondary shifts and positive Cβ secondary shifts indicate a stronger β-sheet conformation.

ences between the incubated and the untreated peptide, suggesting that incubation has less influence on the N-strand structure than the C-strand.

Similar to the ^{13}C spectra, the ^{15}N CP-MAS spectra of [U-F_{12}, V_{14}, G_{17}] PG-1 show pronounced line narrowing and chemical shift changes for the aggregate sample. The most significant line narrowing occurs at G_{17} ^{15}N, while F_{12} undergoes the largest chemical shift change, ~8 ppm upfield as compared to the untreated peptide. Because this change is larger than the typical ^{15}N secondary shift range of Phe,[27] we suspect that it results from the location of Phe ^{15}N at the β-turn, whose chemical shift trend is not as well represented in the protein database as the canonical α-helix and β-sheet structures.

Figure 4 summarizes the line widths (a) and ^{13}C isotropic shift (b) differences between the aggregated and untreated PG-1. The aggregate sample exhibits narrower line widths and stronger β-sheet secondary shifts for most resolved sites, especially for the C-strand residues. For the untreated PG-1, residues in the middle of the strands such as V_{14} and L_5 have narrower lines than terminal residues such as G_{17}. The residue experiencing the most significant ordering is F_{12}, whose Cα and Cβ line widths both decreased, while the terminal G_{17} Cα showed slightly increased disorder in the aggregate. Thus, the β-turn region of the peptide is most strongly structured by incubation. Taken together, the NMR chemical shifts and the microscopy data indicate that the PG-1 aggregates prepared by solution incubation are well ordered on the tens of nanometer scale but do not have the micrometer-length order typical of amyloid fibrils. Because the purpose of this study is to determine the molecular-level packing and hydrogen bonding of PG-1, the nanometer-scale order evident from the NMR line widths and chemical shifts is sufficient for further analysis using 2D ^{13}C correlation experiments.

Packing Motif of PG-1 Aggregates. To determine the packing of PG-1 β-hairpins in the ordered aggregate, we carried out 2D ^{1}H-driven ^{13}C spin diffusion (PDSD) experiments. Figure 5 shows the spectra of [U-F_{12}, V_{14}, G_{17}] PG-1 as 100% labeled aggregates (a), 20% diluted aggregates (b), and untreated 100% labeled peptide (c). A mixing time of 400 ms was used in all experiments to achieve complete exchange. The spectrum of the 100% PG-1 aggregate (Figure 5a) shows significant cross-peaks between F_{12} and V_{14} such as $\alpha-\alpha$, $\alpha-\beta$, and $\alpha-\gamma$. These immediately suggest that the C-strand of one β-hairpin packs closely with another C-strand, causing intermolecular spin diffusion. There are no visible $V_{14}-G_{17}$ cross-peaks and only a weak $F_{12}-G_{17}$ $\alpha-\alpha$ peak, suggesting that the two C-strands are mainly aligned in a parallel fashion. Because the $G_{17}\alpha$ signal is broad and partially overlaps with the $F_{12}\beta$ peak at room

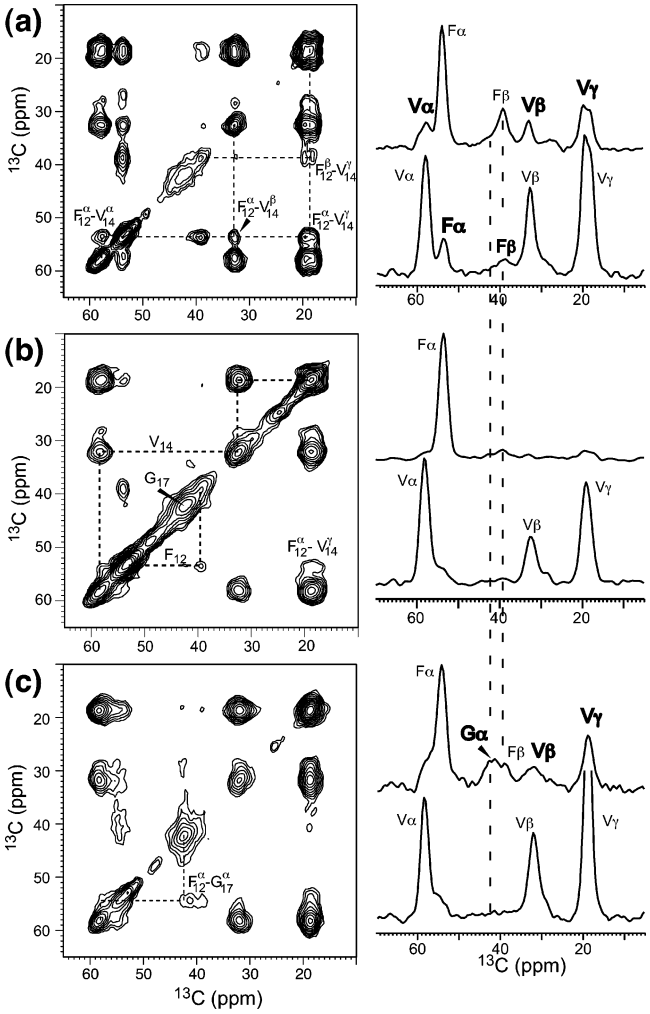

Figure 5. 2D ^{1}H-driven ^{13}C spin diffusion spectra of [U-F_{12}, V_{14}, G_{17}] PG-1. (a) 100% labeled aggregates. (b) 20% labeled aggregates. (c) 100% labeled but untreated peptide. For each 2D spectrum, the 1D cross sections through the $F_{12}\alpha$ (top row) and $V_{14}\alpha$ (bottom row) slices are shown on the right, where inter-residue cross-peaks are indicated in bold.

temperature, we carried out the 2D PDSD experiment on the same sample at 253 K, when the $G_{17}\alpha$ intensity is stronger and better resolved. Under this condition, the $F_{12}\alpha-G_{17}\alpha$ cross-peak decreased even further, to about half the intensity of the room-temperature peak (Table 1), thus confirming that the $F_{12}-G_{17}$ $\alpha-\alpha$ distance is long.

To rule out the possibility that the observed $F_{12}-V_{14}$ cross-peaks are intramolecular, we measured the 2D spectrum of a 20% diluted PG-1 aggregate sample, prepared by co-dissolving 20% labeled peptide with 80% unlabeled peptide in the incubation buffer. Dilution removes intermolecular $^{13}C-^{13}C$ spin diffusion, so that any inter-residue cross-peaks in the spectra must result from intramolecular spin diffusion. Figure 5b shows the 2D spectrum of this diluted sample. Indeed, the $F_{12}-V_{14}$ cross-peaks are either significantly attenuated or disappeared. The only remaining strong cross-peaks are intra-residue ones, confirming that the three labeled residues are sufficiently separated along the β-strand not to cause intramolecular ^{13}C spin diffusion within 400 ms.

To determine whether the NCCN parallel packing of the PG-1 aggregate is specifically caused by incubation, we measured the 2D spectrum of the untreated peptide. The spectrum (Figure 5c) shows much weaker $F_{12}-V_{14}$ cross-peaks but a stronger $F_{12}-G_{17}$ $\alpha-\alpha$ peak. These indicate that in the absence of incubation, PG-1 does not adopt any preferential alignment in the solid state, but has a combination of parallel and antiparallel alignments. The fact that the $F_{12}-G_{17}$ $\alpha-\alpha$ peak is visible while $V_{14}-G_{17}$ cross-peaks are not suggests that it is easier for the two ends of the β-hairpin to contact each other than for the peptide to align in an out-of-registry fashion, which is necessary for forming $V_{14}-G_{17}$ contacts.

Because cross-peaks in the long-mixing-time PDSD experiment can arise from both direct and relay transfer, we carried out a ^{1}H spin diffusion experiment (CHHC) with a short τ_{SD} of 200 μs[18,21] to verify the direct nature of the intermolecular $F_{12}\alpha-V_{14}\alpha$ contact. It has been shown that within a τ_{SD} of ~200 μs, strong cross-peaks in the CHHC spectrum reflect direct $^{1}H-^{1}H$ distances of within ~3 Å.[18,21] Figure 6 shows the CHHC spectra of aggregated (a) and untreated (b) PG-1. The $F_{12}-V_{14}$ $H\alpha-H\alpha$ cross-peak is strong in the aggregate but is absent in the untreated peptide. In fact, the inter-residue $\alpha-\alpha$ cross-peak in the aggregate is higher than some of the intra-residue cross-peaks such as $V\alpha-V\gamma$ (see 1D cross sections in Figure 6c). As compared to the highest intra-residue cross-peak, $F\alpha-F\beta$, which has a distance of ~2.5 Å, the $F_{12}\alpha-V_{14}\alpha$ peak intensity is ~70%, strongly suggesting a direct $F_{12}\alpha-V_{14}\alpha$ distance of ~3 Å.

If the NCCN packing motif is correct, then there should be N-strand to N-strand interfaces in the PG-1 aggregate in addition to the C-strand to C-strand interfaces. To test this, we measured the 2D ^{13}C spin diffusion spectrum of the N-strand labeled aggregate, [U-G_3, L_5] PG-1 (Figure 7a). The spectrum shows well-resolved and clearly visible G_3-L_5 $C'-\alpha$ and $C'-\gamma$ peaks, indicating the existence of short intermolecular distances. Again, the contribution of intramolecular spin diffusion is negligible based on the 2D spectrum of a 20% diluted sample (Supporting Information). Thus, the N-strand does form hydrogen bonds with another N-strand and in a parallel fashion. However, the cross-peaks of the peptide aggregate are not significantly stronger than those of the untreated peptide (Table 1), suggesting that the N-strand is not as tightly packed as the C-strand or that the N-terminus is more disordered than the C-terminus in the aggregate.

The presence of the NCCN packing does not in itself rule out the alternative NCNC packing. To determine if the ordered PG-1 aggregate contains a mixture of NCCN and NCNC packing motifs, we prepared an equimolar mixture of N- and C-strand labeled PG-1 aggregates. If NCNC packing is present, then cross-peaks between the N-strand residues on one molecule and the C-strand residues on another molecule are expected. The 2D spectrum of this mixture is shown in Figure 7b. No N-strand to C-strand cross-peaks such as $V_{14}-L_5$ (dashed circles) and $V_{14}-G_3$ are detected. The only visible intermolecular cross-peaks are the $F_{12}-V_{14}$ peaks due to NCCN parallel packing. These $F_{12}-V_{14}$ peaks are about a factor of 2 weaker than the C-strand sample (Table 1), consistent with the 1:1 molar ratio of the two labeled peptides. Thus, NCCN parallel packing is the sole repeat motif in the ordered PG-1 sample.

Table 1 lists the normalized cross-peak intensities of the 100% N- and C-strand labeled PG-1 aggregates and their untreated equivalents, and of the 1:1 mixture. The cross-peak intensities

Table 1. Cross-Peak Intensities (I_{AB} and I_{BA}) of Aggregated and Untreated PG-1, Normalized with Respect to the Diagonal Peaks (I_{AA} and I_{BB}) According to $I = (I_{AB} + I_{BA})/(I_{AA} + I_{BB})$[a]

cross-peaks		C-strand aggregate		N-strand aggregate	untreated peptide		mixed aggregate
		PDSD	CHHC	PDSD	PDSD	CHHC	PDSD
$F_{12}-V_{14}$	α−α	$0.256^{\pm0.012}$	$0.412^{\pm0.032}$	NA[b]	$0.212^{\pm0.018}$	$0.192^{\pm0.024}$	$0.146^{\pm0.010}$
	α−β	$0.270^{\pm0.014}$	$0.148^{\pm0.022}$	NA	$0.198^{\pm0.024}$	$0.062^{\pm0.026}$	$0.122^{\pm0.010}$
	α−γ	$0.290^{\pm0.010}$	$0.108^{\pm0.026}$	NA	$0.120^{\pm0.006}$	$0.050^{\pm0.014}$	$0.170^{\pm0.006}$
	β−α	$0.200^{\pm0.022}$	$0.256^{\pm0.046}$	NA	$0.088^{\pm0.028}$	$0.080^{\pm0.032}$	$0.190^{\pm0.020}$
	β−β	$0.254^{\pm0.026}$	$0.124^{\pm0.030}$	NA	$0.216^{\pm0.040}$	$0.084^{\pm0.038}$	$0.142^{\pm0.024}$
	β−γ	$0.182^{\pm0.012}$	$0.148^{\pm0.036}$	NA	$0.066^{\pm0.008}$	$0.038^{\pm0.016}$	$0.148^{\pm0.010}$
F_{12}	α−β	$0.506^{\pm0.020}$	$0.596^{\pm0.038}$	NA	$0.380^{\pm0.040}$	$0.460^{\pm0.036}$	$0.282^{\pm0.012}$
V_{14}	α−β	$0.782^{\pm0.022}$	$0.422^{\pm0.028}$	NA	$0.844^{\pm0.026}$	$0.412^{\pm0.028}$	$0.582^{\pm0.018}$
	α−γ	$0.730^{\pm0.012}$	$0.272^{\pm0.034}$	NA	$0.682^{\pm0.008}$	$0.320^{\pm0.014}$	$0.566^{\pm0.010}$
	β−γ	$0.798^{\pm0.014}$	$0.428^{\pm0.026}$	NA	$0.608^{\pm0.008}$	$0.428^{\pm0.016}$	$0.630^{\pm0.010}$
$F_{12}-G_{17}$	α−α	$0.186^{\pm0.018}$ ($0.108^{\pm0.022,c}$)	$0.158^{\pm0.028}$	NA	$0.238^{\pm0.022}$	$0.102^{\pm0.022}$	NA
G_3-L_5	C′−α	NA	NA	$0.086^{\pm0.010}$	$0.086^{\pm0.008}$	NA	NA
	C′−γ	NA	NA	$0.114^{\pm0.006}$	$0.134^{\pm0.008}$	NA	NA

[a] Uncertainties were propagated from the peak intensities and the noise of the 2D spectra. For pure unmixed samples, intensities below ~0.200 are weak cross-peaks reflecting long-range distances. [b] Not applicable. [c] Measured at 253 K.

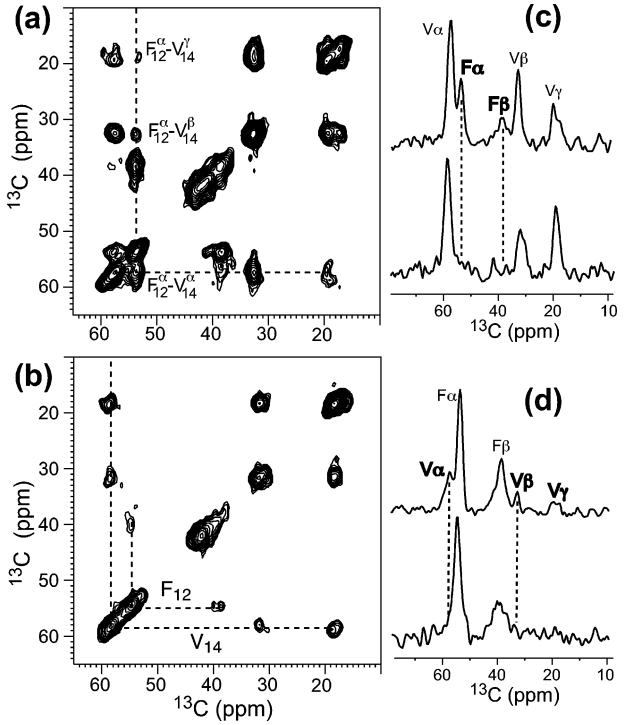

Figure 6. 2D CHHC spectra of (a) aggregated and (b) untreated [U-F_{12}, V_{14}, G_{17}] PG-1. (c) V_{14} Cα cross section for the aggregated (top) and untreated (bottom) peptide. (d) F_{12} Cα cross section for the aggregated (top) and untreated (bottom) peptide. Strong $V_{14}-F_{12}$ cross-peaks (bold) are observed only in the aggregate sample.

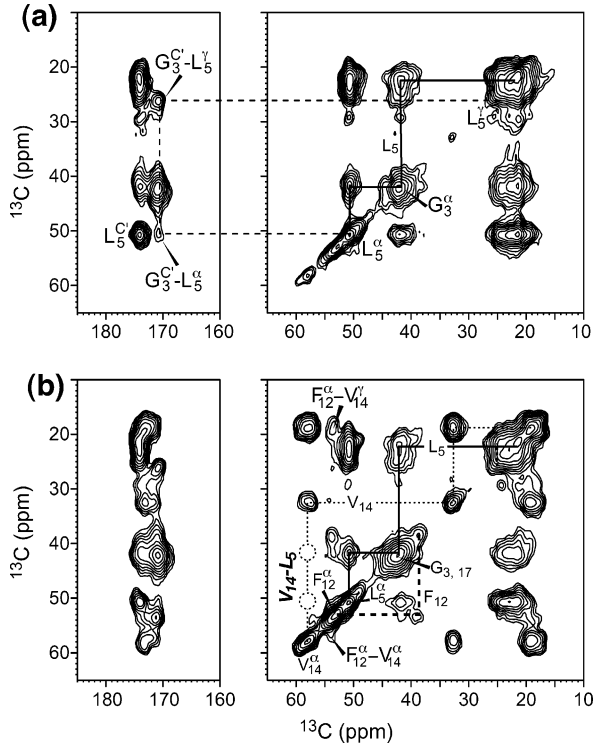

Figure 7. 2D ^{1}H-driven ^{13}C spin diffusion spectra of (a) 100% labeled [U-G_3, L_5] PG-1 aggregates, and (b) 1:1 mixture of [U-G_3, L_5] PG-1 and [U-F_{12}, V_{14}, G_{17}] PG-1 aggregates. Inter-strand cross-peaks such as $V_{14}-L_5$ (dashed circles) are absent in (b).

(I_{AB} and I_{BA}) were normalized to the diagonal peaks (I_{AA} and I_{BB}) according to $I = (I_{AB} + I_{BA})/(I_{AA} + I_{BB})$, and the uncertainties were propagated accordingly from the noise of the 2D spectra. It can be seen that the ordered PG-1 aggregates show significantly stronger C-strand cross-peaks than the untreated peptide in both the PDSD and the CHHC spectra, while the N-strand cross-peaks have more comparable intensities between the two samples. The $F_{12}-V_{14}$ cross-peak intensities in the mixed aggregate are about one-half the intensities of the pure C-strand aggregate, consistent with the fact that only 50% of the C-strand labeled PG-1 is packed next to another C-strand labeled peptide.

Segmental Mobility of PG-1 Aggregates. The ^{13}C line widths of the untreated and aggregated PG-1 samples (Figure 4) indicate that the F_{12} at the β-turn experiences the most significant line narrowing upon aggregation, while the G_{17} Cα signal broadened rather than narrowed, suggesting chain-end disorder in the aggregate. To determine the origin of the order and disorder in the aggregate, we measured the ^{1}H−^{1}H dipolar coupling, ^{13}C−^{1}H dipolar coupling, and ^{1}H $T_{1\rho}$ of untreated and aggregated PG-1. These dynamic parameters are resolved by the ^{13}C isotropic shifts and the use of spin-diffusion free LG-CP. Figure 8 shows the 2D ^{1}H WISE spectrum of the aggregate (a) and its Phe cross sections (solid lines, b), which are superimposed with the cross sections of the untreated peptide

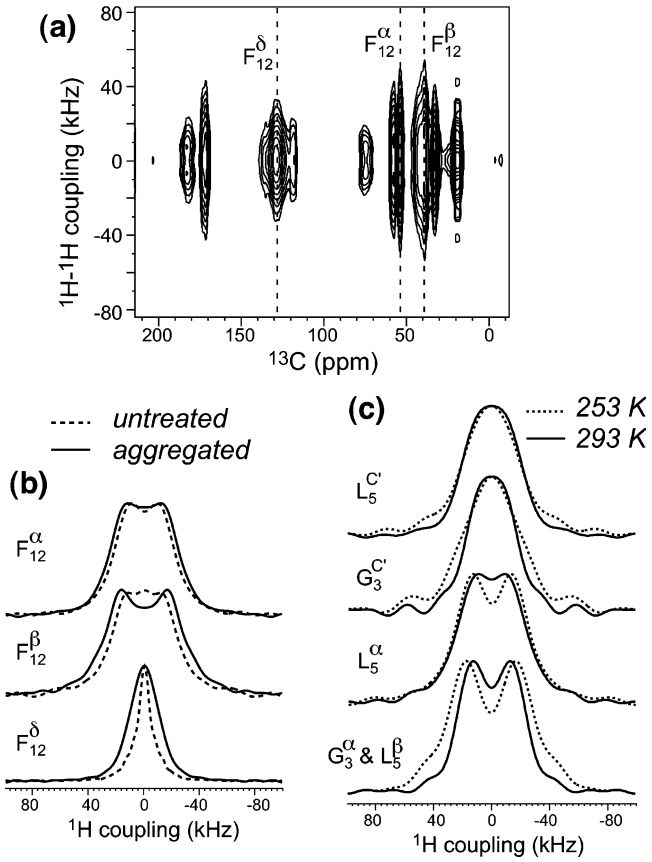

Figure 8. ^{1}H−^{1}H dipolar couplings of PG-1. (a) 2D WISE spectrum of [U-F_{12}, V_{14}, G_{17}] PG-1 aggregates. (b) 1D ^{1}H cross sections of untreated (dashed line) and aggregated (solid line) [U-F_{12}, V_{14}, G_{17}] PG-1. (c) 1D ^{1}H cross sections of [U-G_3, L_5] PG-1 aggregates at 293 K (solid line) and 253 K (dotted line). The backbone dynamics are negligibly unaffected by the temperature, indicating that the N-terminal backbone is immobilized at room temperature.

(dashed lines). The untreated PG-1 exhibits narrower ^{1}H widths than the aggregate, indicating larger-amplitude motion. Moreover, the mobility difference increases down the Phe side chain. Both PG-1 samples are more mobile than amino acid Phe: the latter has an aromatic ^{1}H−^{1}H coupling of 53 kHz, as compared to 25 kHz for the aggregate sample and 9 kHz for the untreated peptide. Cooling the aggregated PG-1 to 253 K increased the ^{1}H−^{1}H couplings but did not completely immobilize the ring (Table 2). Consistently, the ^{13}C−^{1}H dipolar couplings also show that the Phe ring in the untreated peptide undergoes larger-amplitude motion than in the aggregate (Table 2). As compared to F_{12}, no substantial coupling differences are found at G_{17} and V_{14} between the untreated and aggregated samples. Taken together, these indicate that incubation immobilizes the hairpin tip more significantly than the C-terminus.

The ^{1}H $T_{1\rho}$ values of F_{12} Hα and Hβ increased in the aggregate (Table 2), while the $T_{1\rho}$ of G_{17} Hα decreased. These suggest that the broadening of G_{17} Cα signal in the aggregate (Figure 3) results from increased microsecond-time scale motions of the C-terminus, which interfere with CP, while the opposite occurs at F_{12} Cα and Cβ, making the β-turn more ordered and rigid in the aggregate.

Discussion

The NMR line widths and chemical shifts and microscopy images indicate unambiguously that well-ordered PG-1 aggregates on the scale of at least tens of nanometers can be created by appropriate solution incubation. The fact that these aggregates do not show micrometer-length order may result from a combination of the highly charged nature of the peptide and the low aspect ratio of the molecule.

The cross-peak patterns in the 2D ^{13}C correlation spectra indicate that the β-hairpins in the ordered aggregate pack and hydrogen bond in a parallel fashion with like strands facing each other. Both ^{1}H-driven ^{13}C spin diffusion and direct ^{1}H spin diffusion support this conclusion. The ^{13}C spin diffusion experiment detects C−C distances up to ∼7.5 Å within a mixing time of 500 ms, as shown by a recent study of α-spectrin SH3 domain,[29] while the ^{1}H spin diffusion experiment can detect H−H distances within ∼3 Å in a short τ_{SD} of ∼200 μs. Thus, the absence or weakness of ^{13}C spin-diffusion cross-peaks such as F_{12}−G_{17} (Figure 5a) and V_{14}−L_5 (Figure 7b) in the peptide aggregates indicates ^{13}C−^{13}C distances longer than 7.5 Å. These rule out the antiparallel packing and the alternate strand packing (NCNC) models. The strongest constraint in favor of NCCN parallel packing is the significant F_{12}α−V_{14}α cross-peak in the peptide aggregate. Although this cross-peak in the ^{13}C spin diffusion spectrum could arise from both direct and relay transfer, the fact that in the ^{1}H spin diffusion spectrum this α−α peak is stronger than most inter- and intra-residue side chain cross-peaks (Table 1) rules out the possibility of side chain-mediated relay transfer. In addition, the untreated peptide shows clear PDSD intra-residue side chain cross-peaks (Figure 5c) but negligible F_{12}α−V_{14}α intensity, indicating that relay transfer alone is insufficient to produce backbone α−α cross-peaks if the distance is large.

The fact that the N-strand G_3C′−L_5α peak is lower than the F_{12}α−V_{14}α peak in the PDSD spectra is partly due to the larger isotropic shift difference between C′ and Cα, which attenuates ^{13}C spin diffusion. It may also reflect true looser packing of the N-strand interface, which is also manifested in the less dramatic line narrowing of the N-strand residues as compared to the untreated peptide. This looseness likely results from the more hydrophilic nature of the N-strand due to the presence of an additional Arg residue (R_4) in the middle of the strand (Figure 1). In comparison, the C-terminal strand is almost entirely hydrophobic, thus stabilizing the C-strand interface.

Figure 9 illustrates the NCCN parallel packing model of PG-1, showing both a C-strand interface and an N-strand interface. The positions of the neighboring PG-1 molecules are adjusted to satisfy hydrogen-bond lengths, R_{N-O}, of 2.4−3.6 Å.[30,31] Because parallel β-strands do not have an inversion symmetry, each pair of residues has two different internuclear distances across the intermolecular interface. Based on this model, F_{12} and V_{14} have Cα−Cα distances of ∼5 and 10 Å, the shorter of which is the main contributor to the cross-peak in the PDSD spectra. Remarkably, a short F_{12}−V_{14} Hα−Hα distance of ∼3.3 Å is found, confirming that the strong α−α peak in the CHHC spectrum (Figure 6a) is due to direct polarization transfer. At the N-strand interface, a G_3−L_5 C′−Cα distance of ∼6 Å is found, also within the detection limit of ^{13}C spin diffusion. In comparison, the NCCN antiparallel

(29) Castellani, F.; vanRossum, B.; Diehl, A.; Schubert, M.; Rehbein, K.; Oschkinat, H. *Nature* **2002**, *420*, 98−102.
(30) deDios, A. C.; Oldfield, E. *J. Am. Chem. Soc.* **1994**, *116*, 11485−11488.
(31) Creighton, T. E. *Proteins: Structures and molecular properties*, 2nd ed.; W. H. Freeman and Co.: New York, 1993.

Table 2. ^{1}H fwhm of the WISE Spectra, ^{13}C−^{1}H Dipolar Couplings, and ^{1}H $T_{1\rho}$ Values for Aggregated and Untreated PG-1

		^{1}H fwhm (kHz)			^{13}C–^{1}H coupling (kHz)		$T_{1\rho}$ (ms)		
		aggregated		untreated	aggregated	untreated	aggregated		untreated
	site	293 K	253 K	293 K	293 K	293 K	293 K	253 K	293 K
F_{12}	Cα	53	56	47	12	11	5.5	11	3.4
	Cβ	61	70	50	12	11	2.1	8.4	1.6
	Cδ	25	38	9	6.3	3.9	1.6	5.4	2.0
V_{14}	Cα	48	52	50	12	12	7.2	11	6.9
	Cβ	30	38	30	6.6	8.6	4.1	8.6	4.6
	Cγ	11	13	8	2.3	4.3	5.2	9.1	5.8
G^{17}	Cα	52	66	45	11	11	1.5	6.0	2.0

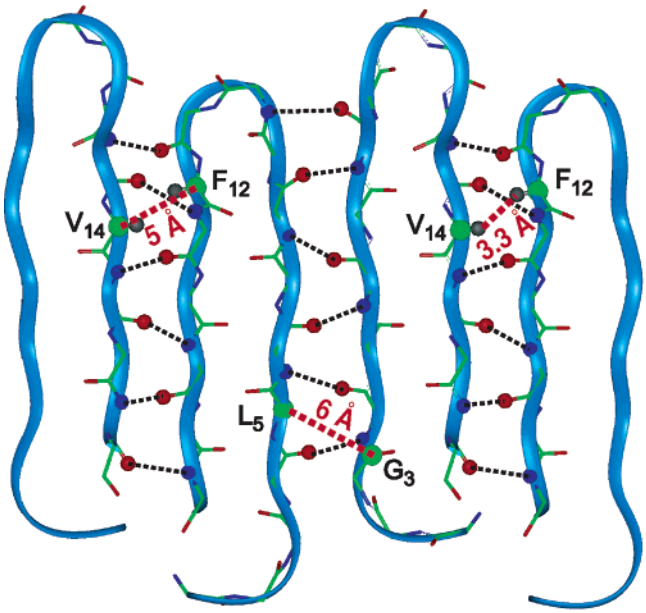

Figure 9. NCCN parallel packing model of PG-1 in the ordered aggregates. Short intermolecular F_{12}−V_{14} and G_3−L_5 Cα−Cα and Hα−Hα distances are highlighted in red. The N−O hydrogen bonds stabilizing the oligomeric structure are shown as black dashed lines.

packing motif yields F_{12}−V_{14} Cα−Cα distances of ∼13 Å, well beyond the detection limit of ^{13}C spin diffusion.

This NCCN packing model shows the direction of the intermolecular contacts to be sideways in the β-hairpin plane rather than perpendicular to the plane. This reflects the fact that the side chains occupy space above and below the β-hairpin plane, which makes it difficult to establish close inter-plane backbone contacts. In amyloid fibrils, the typical distances between adjacent β-sheet planes are 9−10 Å according to fiber diffraction studies.[32,33] Such a large distance is beyond the detection limit of ^{13}C spin diffusion. Moreover, since inter-plane packing is not driven by hydrogen bonding, any accidental close contact between β-sheet planes would be nonspecific in nature; thus the untreated peptide should show similarly strong backbone cross-peaks as the peptide aggregate if inter-sheet contact were the cause of these backbone cross-peaks. This is inconsistent with the experimental data.

The NCCN parallel alignment of PG-1 in the ordered solid-state aggregate determined from these 2D experiments is consistent with the results obtained in the membrane.[34] There, intermolecular C−H, C−N, and C−F dipolar couplings between site-specifically labeled residues constrained the PG-1 dimer structure to be parallel with two C-strands lining the dimer interface. Thus, the PG-1 aggregate formed from solution incubation outside the membrane has similar packing and hydrogen bonding to the membrane-bound PG-1 oligomer. This suggests that the common driving force for the oligomerization of this β-hairpin peptide inside and outside the membrane is hydrogen bonding. This approach of preparing ordered aggregates may thus be useful for studying the oligomerization of other membrane-active β-sheet antimicrobial peptides whose crystal structures are not available.

It is interesting to note that a solution NMR study of PG-1 in DPC micelles[35] showed that the peptide forms antiparallel dimers with the C-strand lining the dimer interface. The reason for the different alignment between the micelle environment, on one hand, and the aggregate and lipid bilayer environments, on the other, is presently unclear. However, because detergent micelles are well known to impose curvature strains onto peptides, one possible reason for the difference may be the different shape anisotropies of the parallel and antiparallel PG-1 dimers. The parallel NCCN packing observed in the aggregate and in the lipid bilayer puts six Arg residues at two adjacent β-turns in close proximity, forming a strongly amphipathic structure. The electrostatic repulsion between these β-turns may make the parallel dimer a bulkier structure than the antiparallel dimer, where the Arg-rich β-turns are spaced apart. The compact antiparallel dimer structure may thus be favored in the constrained micelle environment, while the parallel packing may be stabilized in the bilayer because the stronger amphipathic structure facilitates peptide insertion into the membrane.

Conclusion

We demonstrated the preparation and quaternary-structure determination of well-ordered aggregates of the β-hairpin antimicrobial peptide PG-1. 2D ^{13}C correlation experiments mediated by both ^{13}C and ^{1}H spin diffusion showed intermolecular backbone cross-peaks that are consistent with parallel packing of the β-hairpins, with like strands lining the intermolecular interface. The C-strand interfaces in the aggregate are more tightly packed and ordered than the N-strand interfaces, which may result from the stronger hydrophobic nature of the C-strand. The ordered packing of the aggregate is supported

(32) Jarvis, J. A.; Craik, D. J.; Wilce, M. C. *Biochem. Biophys. Res. Commun.* **1993**, *192*, 991−998.
(33) Malinchik, S. B.; Inouye, H.; Szumowski, K. E.; Kirschner, D. A. *Biophys. J.* **1998**, *74*, 537−545.
(34) Wu, X.; Mani, R.; Buffy, J. J.; Tang, M.; Waring, A.; Hong, M., submitted.
(35) Roumestand, C.; Louis, V.; Aumelas, A.; Grassy, G.; Calas, B.; Chavanieu, A. *FEBS Lett.* **1998**, *421*, 263−267.

by the reduced mobility of the Phe ring at the β-turn as compared to the untreated peptide. This is the first time a β-hairpin peptide is shown to be able to form ordered aggregates on the length scale of tens of nanometers. The hydrogen-bonding propensity of PG-1 in the solid state determined from this study sheds light on the oligomerization of this peptide in lipid bilayers, which will be presented elsewhere.[34]

Acknowledgment. We thank Dr. Tracey M. Pepper for help in the electron microscopy measurements. This work is supported by the National Institutes of Health grant GM-066976 to M.H. and grants AI-22839 and AI-37945 to A.J.W.

Supporting Information Available: 2D ^{13}C correlation spectra of [U-F_{12}, V_{14}, G_{17}] PG-1 aggregates at 253 K and of 20% diluted [U-G_3, L_5] PG-1. This material is available free of charge via the Internet at http://pubs.acs.org.

JA0526665

Supporting Information

Intermolecular Packing and Alignment in an Ordered β-Hairpin Antimicrobial Peptide Aggregate from 2D Solid-State NMR

Ming Tang[a], Alan J. Waring [b], and Mei Hong [a]*

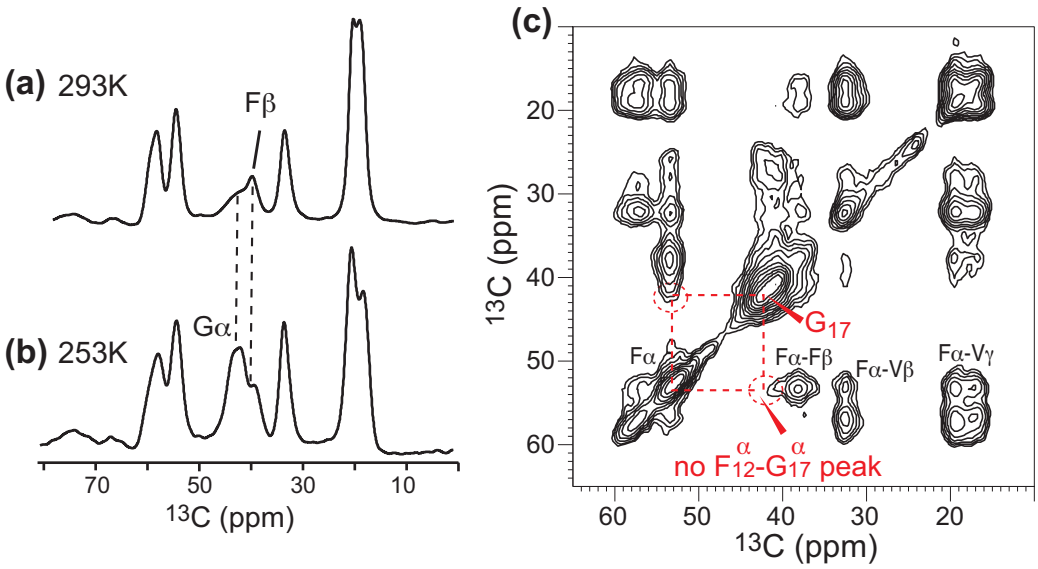

Figure S1. Lack of F_{12}-G_{17} α–α cross peak in the 100% [U-F_{12}, V_{14}, G_{17}] PG-1 aggregate at 253 K. (a) 1D ^{13}C spectrum of the peptide at 293 K. (b) 1D ^{13}C spectrum of the peptide at 253 K. The G_{17}α peak has higher intensity and is better resolved from the F_{12}β signal at 253 K. (c) 2D ^{13}C spin diffusion spectrum of the peptide aggregate at 253 K with a mixing time of 400 ms. Despite the prominent diagonal G_{17}α peak, the F_{12}-G_{17} α-α cross peak is negligible (dashed circles), confirming that the C-strands are aligned in a parallel fashion in the aggregate.

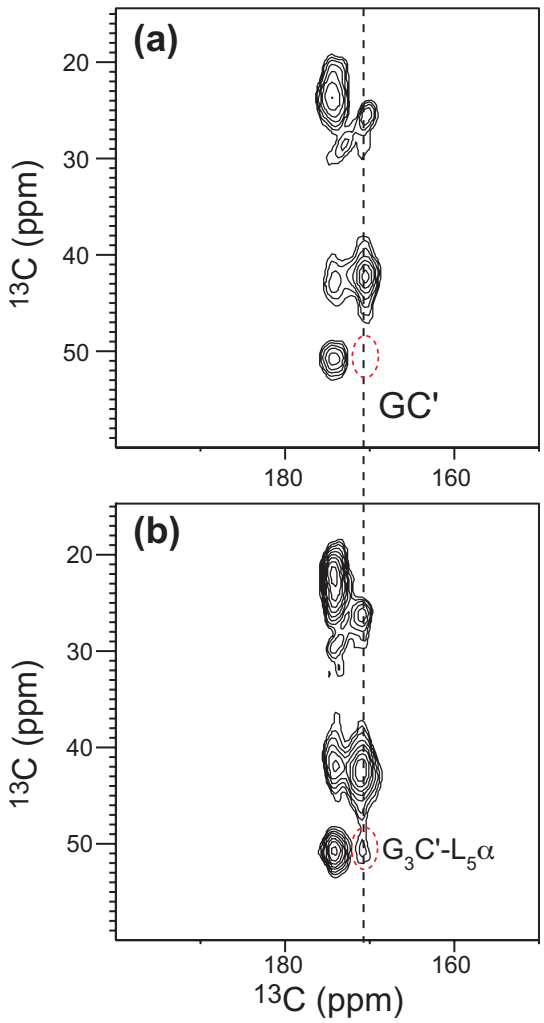

Figure S2. (a) 2D ^{13}C PDSD spectrum of 20% diluted and untreated [U-G_3, L_5] PG-1 at 293 K. Negligible G_3-L_5 C'-Cα cross peak is observed. (b) PDSD spectrum of the 100% [U-G_3, L_5] PG-1 aggregate is reproduced from Figure 7(a), where a clear G_3-L_5 C'-Cα cross peak is observed.